

Development of a Nitrogen Dioxide Gas Sensor Based on Mid-Infrared Absorption Spectroscopy

Hiroaki ASHIZAWA, Shigeru YAMAGUCHI, Masamori ENDO, Shinobu OHARA,
Masao TAKAHASHI, Kenzo NANRI, and Tomoo FUJIOKA

Department of Physics, School of Science, Tokai University, 1117 Kitakaname, Hiratsuka, Kanagawa, 259-1292

(Received October 18, 2002)

We demonstrated a mid-IR optical NO₂ monitor based on a frequency-stabilized, Yb-fiber laser pumped difference frequency generation (DFG) in a periodically poled lithium niobate (PPLN) crystal. A high power Yb-fiber laser with a fiber Bragg grating (FBG) and a distributed feedback (DFB) laser diode were used as DFG pump and signal sources, respectively. The spectral characteristics of NO₂ were evaluated using a multipass absorption cell with an optical path length of 10 m. Continuous absorption spectra of NO₂ from 2886.5 cm⁻¹ (3.464 μm) to 2896.5 cm⁻¹ (3.452 μm) were demonstrated over 10 cm⁻¹ with a spectral resolution of approximately 60 MHz. We also demonstrate reproducibility and stability of NO₂ detection system with the mid-IR light sources were investigated, in addition to long-term monitoring of NO₂ concentrations over a three-day period.

Key Words: Fiber laser, Difference-frequency generation, Laser spectroscopy, NO₂ detection, PPLN crystal.

1. Introduction

Highly sensitive and selective monitoring of numerous gas species has become increasingly important and necessary in various fields for environmental trace gas monitoring, industrial plant surveillance and process control. Various trace gas monitoring technologies have been classified into two categories: the non-optical chemical method and the optically-based method.

Desirable performance characteristics for recent gas sensors are: fast temporal response, high selectivity of particular species, long-term stability without maintenance and re-calibration and real time measurement in just a few seconds. In light of such requirements, tunable continuous-wave narrow-linewidth laser-based absorption spectroscopy methods are highly advantageous and have been applied for trace gas detection in situations such as industrial plants, environmental monitoring and process control. Moreover, laser-based spectroscopy can be used to observe radical chemical changes in gases. In particular, infrared absorption spectroscopy is a convenient and useful technique that is applied to many environmental trace gas species, because most such environmental molecules have overtone and fundamental ro-vibrational absorption lines in the near-IR and mid-IR regions. The near-IR region, from 1 μm to 2 μm, usually belongs to the first and second overtone bands, and it can be accessed directly by a several mill-watt III-V semiconductor diode laser.¹⁻⁴⁾ However, first- and second- overtone band transition strengths are one to two orders of magnitude weaker than fundamental ro-vibrational absorption lines. Therefore, a tunable cw narrow linewidth light source in the mid-IR region is used for high sensitive laser absorption spectroscopy.

Fourier transform infrared (FTIR) spectrometers can detect a wide spectral range (> 2000 cm⁻¹) in a few seconds, however,

typical resolution of such instruments is ~ 0.1 cm⁻¹ (3 GHz). To improve the resolution, lead salt based diode lasers, and more recently quantum cascade (QC) laser diodes have been developed as cw mid-IR coherent sources. Such light sources in the mid-IR region apply to highly sensitive trace gas detection.^{5,6)} However, cryogenic cooling with a sensitive temperature control for trace gas detection is required.

For the accessible wavelength region from 2 μm to 5 μm and the obtained narrow linewidth light source, we used a difference frequency generation (DFG) technique.^{7,8)} The DFG technique is a very convenient one that mixes two near-IR laser sources (λ_1, λ_2) to generate mid-IR ($\lambda_3 = (1/\lambda_1 - 1/\lambda_2)^{-1}$) in a quasi-phase-matched (QPM) nonlinear optical crystal of a periodically-poled LiNbO₃ (PPLN) with a single-pass geometry. The generated wavelength range of DFG is mainly determined by the transparency range of the nonlinear optical material transparent range from 0.4 μm to 5.0 μm.⁹⁾

Generally, generated mid-IR light depends strongly on the two near-IR laser source characteristics. In this work, as one of the pump sources for DFG, we used a compact Yb-doped fiber laser with a fiber Bragg grating (FBG), which can be operated at room temperature. A high power Yb-fiber laser with an FBG can be generated with an output power of up to ~ 1 W with a single spatial mode around the 1-μm region.¹⁰⁻¹²⁾ Moreover, one of the advantages of fiber lasers with an FBG, is that the center wavelength can be easily selected by adjusting the FBG parameter in the range of 1035 to 1120 nm, which corresponds to the Yb-doped fiber amplifier gain region. The other laser used was a compact tunable telecommunication DFB laser diode that can be selected in a standardized International Telecommunication Union (ITU) 50 GHz spaced frequency grid in a range of 1260 ~ 1360 nm (O-band), 1360 ~ 1460 nm (E-band), 1460 ~ 1530 nm

(S-band), 1530 ~ 1565 nm (C-band), 1565 ~ 1625 nm (L-band) and 1625 ~ 1675 nm (U-band). Therefore, the mid-IR range from 2.6 μm to 4.5 μm becomes readily accessible by selecting an Yb-fiber laser wavelength from 1035 nm to 1120 nm together with a tunable DFB telecommunication laser diode from 1260 nm to 1675 nm, resulting in an excellent wavelength tuning flexibility. In a previous study, we have reported DFG characteristics at 3.3 μm such as polarization stability, center wavelength stability, DFG slope efficiency and spectral linewidth.¹³⁾

Our motivation is to develop a compact and rugged “difference-frequency” technique based on a trace gas sensor that is widely tunable in order to detect many other gas species. In this paper, we report the performance of the fiber-laser-based NO₂ gas sensor for sensitive and real time measurement. There are three fundamental ro-vibration bands of NO₂ lines absorbing at 3.5 μm , 6.2 μm , and 13.3 μm . We selected the $\nu_1 + \nu_3$ band of NO₂ absorption spectrum lines around 3.5 μm .^{14,15)} In the 3.5- μm region, the NO₂ absorption line is about 20 times weaker than the absorption line in the 6.2- μm region; however, the former region can be easily found by using a “difference-frequency” technique. This region is relatively free of interference from H₂O and other gases. An Yb-fiber laser (200 mW wavelength at 1064 nm) and a DFB laser diode (20 mW wavelength at 1536 nm) were incorporated with the DFG pump and signal sources, respectively. The sensor could detect NO₂ gas concentrations up to 1500 ppm with a quick response time. The DFG wavelength tunability and performance of the detected NO₂ spectrum was evaluated using a gold-coated multipass gas absorption cell with an optical path length of 10 m.

2. Experimental detail

A schematic diagram of the mid-IR with a 3.5- μm DFG spectroscopic source and a NO₂ gas detection system is shown Fig. 1. This NO₂ gas sensor system consists of three stages; a DFG pump stage, a DFG generation stage and a gas detection stage. In the nonlinear DFG process, the two incident waves, which are customarily called pump (ω_p) and signal (ω_s) waves, are down-converted to generate the idler beam (ω_i) in accordance with the relation $\omega_i = \omega_p - \omega_s$. As mentioned above, the key components for generating the mid-IR spectroscopic source are two compact single-mode fiber pigtailed near-IR pump and signal sources. As the DFG pump source, we used a frequency-

stabilized Yb-doped fiber laser with an FBG. The fiber laser consists of an FBG-stabilized seed laser oscillator stage and an Yb fiber amplifier stage with double cladding specially designed for this study. This fiber laser can be operated at an output power of 200 mW with a center wavelength of 1064 nm. The DFG signal source is a frequency-tunable DFB laser diode (NTT Electronics Inc. Model: NLK1554STB), which is used in the telecommunication field. This DFB laser diode can be operated with output power of 20 mW, a center wavelength of 1536 nm \pm 2 nm, and a linewidth of approximately 1 MHz. The DFB laser diode frequency can be varied by $\sim 0.02 \text{ cm}^{-1}/\text{mA}$ with an injection current and $\sim 0.35 \text{ cm}^{-1}/\text{K}$ with temperature modulation. A three-port wavelength division multiplexer (WDM) is used to combine the above-described pump and signal near-IR laser sources. To prevent the refraction noise at the end of each fiber, two near-IR laser sources are directly fusion-spliced to the WDM. The fiber connection between each laser source and the WDM causes a power loss due to connection losses from fusion-splicing and loss related to miss-match in the mode field diameter of each fiber.

To investigate the WDM's insertion losses, we compared the direct output power and past-fusion-spliced output power of each laser source. The insertion losses of pump and signal lasers investigated were 15 % and 8 %, at 1064 nm and 1536 nm, respectively. In-line compact polarization controllers (General Photonics Inc, Model: PLC-003) are inserted after pump and signal sources in each delivery fiber. These polarization controllers are employed to set the linear and vertical polarization for the $e + e \rightarrow e$ interaction in periodically-poled LiNbO₃ which provide access to the highest nonlinear coefficient of lithium niobate. The pump and signal beams are emitted into free space from the 8° angled polished coupler (APC) fiber end. The emitted beams have a Gaussian spatial profile and they are focused into the center of the PPLN crystal with a diameter approximately 80 μm by an anti-refraction (AR) coated achromatic lens (New port Inc. Model: N-20X-APO-IR, $f = 10 \text{ mm}$ $N.A. = 0.35$). The PPLN crystal used in this experiment was 20.5 mm long and 0.5 mm thick, with 10 grating channels with periods ranging from 29.6 μm to 30.5 μm , in increments of 0.1 μm and 0.88 mm wide for each channel.

The PPLN nonlinear crystal temperature was controlled by a Peltier thermo-electric element to optimize the phase matching condition. A phase matching condition calculated from

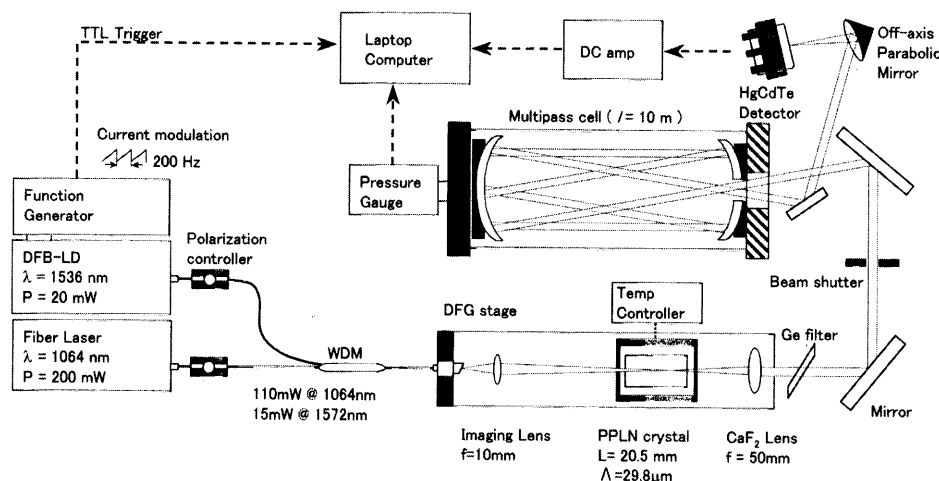


Fig. 1 Schematic of a mid-IR 3.5 μm spectroscopic DFG source configured for NO₂ gas detection.

Sellmeier's equation, $n_3/\lambda_3 = n_1/\lambda_1 - n_2/\lambda_2 - 1/\Lambda$ (where Λ is the grating period and n_1 , n_2 and n_3 are the extraordinary refraction indices),¹⁶⁾ and such conditions were obtained at the 29.8 μm grating channel period where a calculated temperature of 297 K was obtained. The mid-IR DFG radiation from the PPLN crystal was collimated by an $f=50$ mm uncoated calcium fluoride (CaF_2) convex lens. The unconverted residual pump and signal beams were blocked by a 0.8-mm thick, AR-coated germanium filter. To perform the absorption spectrum, we used a gold-coated astigmatic Herriott multipass absorption cell (0.3-liter volume) fitted with a CaF_2 window. The cell was configured for 41 passes, corresponding to an optical path length of approximately 10 m, and had a measured transmission of approximately 50 %. After the DFG-proved beam passed through the multipass cell, it was focused into a low-noise HgCdTe (MCT) detector with a 1 mm^2 active area by using a gold-coated off-axis parabolic mirror with a focal length 50.4 mm. The MCT detector operates in a photoconductive mode and is cooled down to 200 K by a three-stage thermo-electric cooler. The detected signal is amplified by a DC amplifier.

The detected signals were recorded by a laptop computer fitted with a data acquisition card (National Instruments. Model: DAQ card-AL-16XE-50), with a 200-kS/s sampling rate and 16-bit resolution. A data acquisition card is used to acquire the absorption and pressure transducer signals. This card also controls a mechanical shutter and evaluates background light and thermal noise occurring during the experiment condition. In order to calculate an absolute spectroscopic absorption measurement, it was necessary to subtract background noise from the detected signal, including the absorption spectrum. To monitor sampling gas pressure fluctuations during measurement, a miniature in-line pressure gauge was used to measure the real-time gas pressure of the multipass absorption cell.

3. Results and discussion

3.1 Pump and signal laser characteristics

(a) Fiber laser characteristics

It is necessary to verify whether a fiber laser with an FBG can be sufficiently stable to act as a pump laser for a DFG spectroscopic source. Thus, we investigated the fiber laser's operating characteristics, such as center frequency drift and polarization stability induced by changes in ambient temperature conditions. To investigate fiber laser polarization stability, a polarizer was placed between the fiber laser and a Si detector (NEW Focus Inc. model: 2033). The relative power was measured as a function of the polarizer's adjustment angle. The polarization characteristics were examined with the same experimental set up described in detail.¹⁷⁾ To investigate the fiber laser center frequency stability as a function operation time in ambient temperature conditions, the high-resolution wavemeter (Burleigh WA-1500NIR ± 0.002 cm^{-1} absolute accuracy) was used. This result is shown in Fig. 2. The center frequency drift was found to be less than ± 100 MHz after 60 min of warming up time. We used a Michelson interferometer to estimate the actual fiber laser linewidth. Because the interferometer's vision disappeared when the optical path difference of the two arms was 7.3 m, the fiber laser linewidth was estimated to be 44 MHz.

(b) DFB Laser Diode Characteristics

The effective tuning range for changes in temperature and injection current were measured using a high-resolution wavemeter, with results shown in Fig. 3. The DFB laser diode

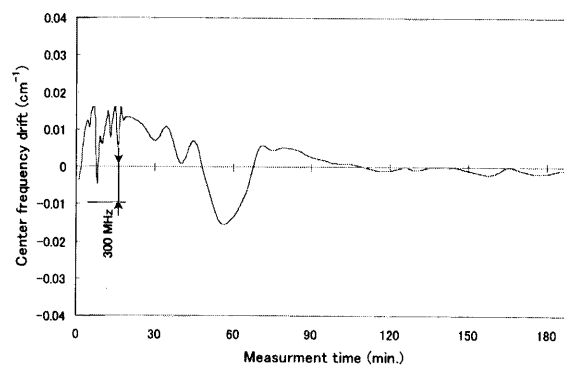


Fig. 2 Frequency stability evaluation of fiber laser with FBG. This figure indicates the center frequency drift of fiber laser results within ± 100 MHz, after the 60 min warm-up period.

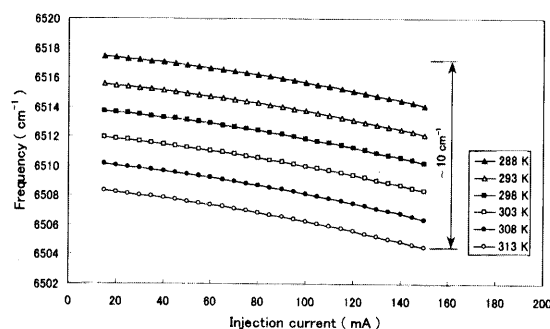


Fig. 3 DFB laser diode (signal source) frequency tuning characteristics with injection current and temperature modulation. This DFB laser diode can be adjusted to range from ~ 6517.4 cm^{-1} to ~ 6504.1 cm^{-1} and a maximum tuning range of over 10 cm^{-1} .

frequency can be varied by ~ 0.02 cm^{-1}/mA with injection current and ~ 0.35 cm^{-1}/K with temperature control. This DFB laser diode can be adjusted with a range between ~ 1534.35 nm (~ 6517.4 cm^{-1}) and ~ 1537.5 nm (~ 6504.1 cm^{-1}), with and temperature control ranging from 288 K to 313 K. The maximum tuning range was found to be approximately 10 cm^{-1} with injection current and temperature control without any mode hops.

3.2 DFG characteristics and spectroscopic performance

The 3.5- μm mid-IR radiation was generated for wavelengths of 1064 nm and 1532 nm using a PPLN crystal with a 29.8 μm period. Using the described DFG generation system, we measured a DFG radiation of ~ 1.35 μW at ~ 3.5 μm , with incident power of 110 mW and 15 mW at 1064 nm and 1536 nm, respectively. Measurements of the mid-IR power were used, taking into account reflection losses at the surfaces of the CaF_2 collimation lens and Ge filter of 8 % and 9.5 %, respectively. The DFG slope efficiency is evaluated to be 0.82 mW/W^2 . The mid-IR power attenuated to approximately 0.5 μW on the MCT detector after passing through the absorption multipass cell in this experimental setup.

To investigate the performance of this detection system, we tested several absorption spectrum lines in the $\nu_1 + \nu_3$ band of NO_2 at around 3.5 μm . To calibrate the equipment, we used a reference gas that contained NO_2 at a concentration specified to be 436 ppm. A spectroscopically important characteristic of trace gas optical absorption monitoring system is that it enables us to

access the particular absorption line of the selected target gas species. Figure.4 (a) shows demonstrated continuous NO₂ absorption lines around ~2893 cm⁻¹, obtained by wide frequency scanning of the DFG spectroscopic source in this experiment. In order to obtain a continuous absorption spectrum, a DFB laser diode was applied for injection current and temperature modulation. The DFG spectroscopic source frequency tuning range from 2886.5 cm⁻¹ (3.464 μm) to 2896.5 cm⁻¹ (3.452 μm) is demonstrated to be 10 cm⁻¹ (~ 300 GHz) in this experiment, measured absorption line transition and position using a multipass absorption cell containing approximately 436 ppm of NO₂ at 13 kPa and 298 K. Several NO₂ absorption lines exist in this 3.5 μm region. Operating at reduced pressure improves the selectivity by reducing the pressure broadening without affecting concentration measurements, and it decreases overlap from other NO₂ spectra. This figure shows that DFG spectroscopic sources can be continuously tuned without any frequency mode hops. Figure. 4 (b) shows the expected NO₂ absorption lines close to 2893 cm⁻¹ with the same condition as used in the experimental comparisons obtained from the HITRAN 96 database.¹⁸⁾ The result shows that observed NO₂ absorption strength and position were in good agreement with simulated NO₂ absorption spectra from the HITRAN 96 database.

Figure. 5 shows NO₂ absorption lines around 2892.5 cm⁻¹ (3.457 μm) which from part of the continuous NO₂ absorption spectrum (as shown in Fig. 4 (a)). To investigate the resolution of this detection system, we selected on NO₂ absorption spectrum at 2893.013 cm⁻¹ and a cell pressure of 400 Pa (Fig. 4 in column). The frequency of the DFG spectroscopic source is scanned at 0.14 cm⁻¹ (~ 4.2 GHz) by applying injection current modulation with a DFB laser driver. Here, the minimum spectral resolution was 1.84×10^{-4} cm⁻¹ (~ 5.5 MHz). The linewidth for the observed NO₂ spectrum at 2893.013 cm⁻¹ was measured to be 172 MHz (FWHM). The theoretical NO₂ Doppler absorption spectrum linewidth value of 161 MHz was calculated from the HITRAN 96 database. Thus, the linewidth of the DFG probe beam is estimated to be approximately 62 MHz from deconvoluting the calculated and recorded.

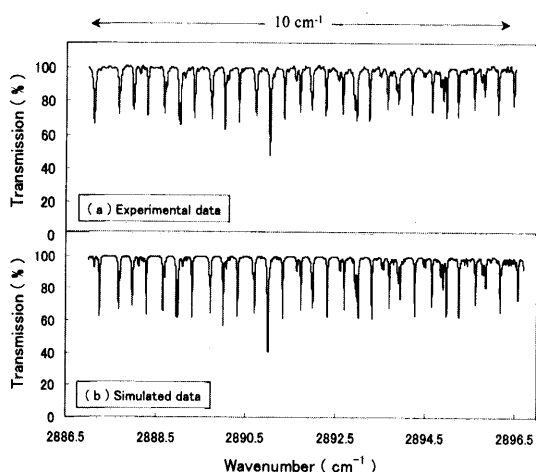


Fig. 4 (a) Experimental continuous NO₂ absorption spectrum lines around ~ 2893 cm⁻¹ at a cell pressure of 13 kPa and an optical path length of 10 m. (b) Simulated continuous NO₂ absorption spectrum lines around ~ 2893 cm⁻¹ from HITRAN96 database under the same conditions as used in the experiment.

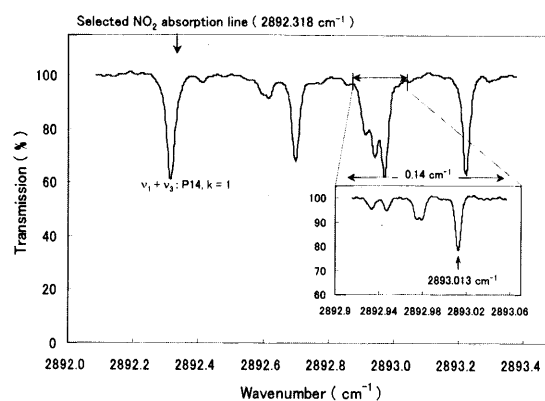


Fig. 5 Experimental NO₂ absorption spectrum around 2892.318 cm⁻¹ at a cell pressure of 13 kPa. The inset shows a high resolution NO₂ absorption spectrum at 2893.013 cm⁻¹ and a cell pressure of 400 Pa.

3.3 NO₂ measurement

An absorption line at 2892.318 cm⁻¹ was selected for NO₂ concentration measurements. To calculate the NO₂ concentration, we need to estimate the line intensity of observed NO₂ absorption spectrum due to two completely overlapping absorption spectrum lines at 2892.3179 cm⁻¹ and 2892.3183 cm⁻¹. The discrepancy between the two absorption spectra's center positions is approximately 4.19×10^{-4} cm⁻¹, which is much less than the resolution limit of this system. To estimate the temperature-dependent line intensity ($S(T)$: cm molecules⁻¹) of the observed spectrum, we used the following equation:

$$S(T) = \frac{\alpha(\nu)}{g(\nu - \nu_0)N_L} \quad (1)$$

where $g(\nu - \nu_0)$ is the normalized, pressure-dependent lineshape function. Here, N is the total number of molecules of absorbing gas. The value of N at 296 K is Loschmidt's number, $N_L = 2.479 \times 10^{19}$ [molecules cm⁻³ atm⁻¹]. The parameter $\alpha(\nu)$ is the linear absorption coefficient [cm⁻¹ atm⁻¹] calculated by Lambert-Beer's law. Based on this analysis, we calculated the molecular line intensity from the measured absorption spectrum and estimated it to be 8.77×10^{-21} cm/molecule. This estimated experimental line intensity value was in good agreement with the simulated line intensity from the HITRAN 96 database, which was of 9.17×10^{-21} cm/molecule. This result shows that estimated DFG linewidth has little influence on the actual absorption spectrum measurement. The minimum detectable concentration (MDC) value was estimated to be approximately 5 ppm to measure this absorption line, and assuming the $S/N = 1$, an absorption measurement sensitivity of $\pm 1.5 \times 10^{-3}$, for a maximum averaging time of 10 sec.

When measuring NO₂, we should consider the equilibrium for the gaseous dissociation/association reaction between N₂O₄ and NO₂.¹⁹⁾ The nitrogen dioxide tends to dimerize, and the equilibrium reaction with the dimer (dinitrogen tetroxide) is expressed by the following chemical formula:



It is well known that NO₂ significantly dimerizes at slight temperature variations. Consequently, the partial pressures of the monomer and dimer both contribute to the measured total pres-

sure. The degree of dissociation between P_{NO_2} and $P_{\text{N}_2\text{O}_4}$ can be expressed by the following equation:

$$\alpha = \sqrt{\frac{\kappa_p}{4P_{\text{total}} + \kappa_p}} \quad P_{\text{N}_2\text{O}_4} = \frac{1-\alpha}{1+\alpha} P_{\text{total}}$$

$$P_{\text{NO}_2} = \frac{2\alpha}{1+\alpha} P_{\text{total}} \quad (3)$$

where α is the degree of dissociation, P_{total} is the total pressure in the cell, which includes both the contribution from the monomer and the dimer, and κ_p is the equilibrium constant. Here, the value κ_p has a temperature dependence that results in a decrease/increase in the dimerization fraction with increasing/decreasing sample gas temperature.²⁰⁾ This effect, in conjunction with the decrease in sample density as a function of increasing temperature, leads to an extremely weak temperature dependence on the NO_2 density. Based on this analysis, we attempted to calculate influence of dimerization as a function of the sample gas temperature. The total pressure in the 1000 ppm cell includes both contributions from the monomer and dimer. The density of NO_2 in the sample cell changes by approximately 5.0 % over a temperature range of 260 – 265 K. The partial pressure of the monomer was then calculated as $P_{\text{NO}_2} = 950$ ppm at 260 K. Furthermore, this calculation shows that the dimer began to influence the measurement of NO_2 concentration at temperatures less than approximately 280 K.

To investigate the overall instrument performance, which includes reproducibility and stability of the detection system for long-term measurements, was assessed by monitoring the NO_2 line at 2892.318 cm^{-1} . In this long-term test, a calibrated NO_2 (436 ppm) sample and dry air alternately flowed through into the multipass cell at a pressure of 13 kPa. To prevent the influence of the dimerization fraction as a function of temperature, we set the sample gas temperature at 297 K in this measurement. The NO_2 concentration measurement for a part of the three-day period is shown in Fig. 6. As calibrated NO_2 flowed into the multipass cell, the gas sensor measured a concentration of ~ 450 ppm, which is within about 3.0 % of the calibrated concentration (this concentration measurement used the estimated line intensity of $8.77 \times 10^{-21} \text{ cm/molecule}$ for the observed NO_2 absorption line at 2892.318 cm^{-1}). The measurement standard deviation was estimated to be ± 5.3 ppm, which corresponds to absorption sensitivities of $\pm 1.5 \times 10^{-3}$ (Fig. 6 in column).

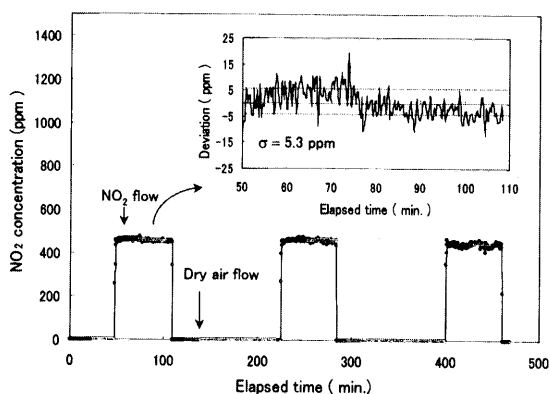


Fig. 6 Calibrated NO_2 concentration monitoring over an extended time period.

4. Conclusions

A frequency-stabilized, Yb-doped fiber laser-pumped DFG in a PPLN crystal based portable NO_2 sensor was developed. We achieved a mid-IR power of $\sim 1.35 \mu\text{W}$ at $3.5 \mu\text{m}$ with a slope efficiency of 0.82 mW/W^2 . These results suggest that the FBG-tuned Yb-fiber laser can be identical to other DFG pump sources from the perspective of slope efficiency. A continuous absorption spectrum of NO_2 from 2886.5 cm^{-1} ($3.464 \mu\text{m}$) to 2896.5 cm^{-1} ($3.452 \mu\text{m}$) was demonstrated to be 10 cm^{-1} with a spectral resolution of 62 MHz. We also demonstrated real-time detection of a doubled NO_2 line at 2892.218 cm^{-1} by monitoring a calibrated of sample NO_2 (436 ppm) over a three-day period and measuring a concentration of 450 ppm with standard deviation of ± 5.3 ppm.

Such results suggest that the narrow linewidth fiber laser with an FBG can serve as an efficient pump source instead of either a frequency-stabilized LD-pumped Nd:YAG laser or intense DFB laser diodes. This DFG source is applied to NO_2 detection, which is of interest in various applications in combustion, environmental, and trace gas monitoring.

References

- 1) H. Sasada, S. Takeuchi, M. Iritani, and K. Nakatani: *J. Opt. Soc. Am. B* **8** (1991) 713.
- 2) K. Uehara and H. Tai: *Apl. Opt.* **31**(1992) 809.
- 3) M. E. Webber, S. Kim, S. T. Sanders, D. S. Baer, R. K. Hanson, and Y. Ikeda: *Appl. Opt.* **40** (2001) 821.
- 4) M. E. Webber, D. S. Baer, and R. K. Hanson: *Appl. Opt.* **40** (2001) 2031.
- 5) J. Reid, J. Shewchun, B. K. Garside, and E. A. Ballik: *Apl. Opt.* **17** (1978) 300.
- 6) A. A. Kosterev, F. K. Tittel, C. Gmachl, F. Capasso, D. L. Sivco, J. N. Baillargeon, A. L. Hutchinson, and A. Y. Cho: *Apl. Opt.* **39** (2000) 6866.
- 7) A. Balakrishnan, S. Sanders, S. DeMars, J. Webjörn, D. W. Nam, R. J. Lang, D. G. Mehuys, R. G. Waarts, and D. F. Welch: *Opt. Lett.* **21** (1996) 952.
- 8) D. Mazzotti, P. De Natale, G. Giusfredi, C. Fort, J. A. Mitchell, and L. W. Hollberg: *Appl. Phys. B* **70** (2000) 747.
- 9) Martin M. Fejer, G. A. Magel, Dieter H. Jundt, and Robert L. Byer: *IEEE J. Quant. Electron.* **28** (1992) 2631.
- 10) H. M. Pask, R. J. Carman, D. C. Hanna, A. C. Tropper, C. J. Mackechnine, P. R. Barber, and J. M. Dawes: *IEEE J. Sel. Top. Quant. Electron.* **1** (1995) 2.
- 11) H. M. Pask, J. L. Archambault, D. C. Hanna, L. Reekie, P. St. J. Russell, J. E. Townsend, and A. C. Tropper: *Electron. Lett.* **30** (1994) 863.
- 12) J. Y. Allain, J. F. Bayon, M. Monerie, P. Bernage, and P. Niay: *Electron. Lett.* **29** (1993) 309.
- 13) H. Ashizawa, S. Ohara, S. Yamaguchi, M. Takahashi, M. Endo, K. Nanri, T. Fujioka, and F. K. Tittel: to be published in *Jpn. J. Appl. Phys.*
- 14) R. A. Toth and R. H. Hunt: *J. Mol. Spectrosc.* **79** (1980) 182.
- 15) A. Perrin, J. M. Flaud, and C. C. Peyret: *Infrared. phys.* **22** (1982) 343.
- 16) D. H. Jundt: *Opt. Lett.* **22** (1997) 1553.
- 17) N. Matsuoka, S. Yamaguchi, K. Nanri, T. Fujioka, D. Richter, and F. K. Tittel: *Jpn. J. Appl. Phys.* **40** (2001) 625.
- 18) HITRAN96, Ontar Corporation, North Andover, MA, USA.
- 19) T. M. Stephen, A. Goldman, A. Perrin, J. M. Flaud, F. Keller, and C. P. Rinsland: *J. Mol. Spectrosc.* **201** (2000) 134.
- 20) M. H. Harwood and R. L. Jones: *J. Geophys. Res.* **99** (1994) 955.